

NO. 39. ANALYSIS OF LUNAR LINEAMENTS, I: TECTONIC MAPS OF THE MOON

by ROBERT G. STROM

July 1, 1964

ABSTRACT

Lineaments within 60° of the moon's center of face have been mapped in detail. Four global lineament systems and radial systems associated with four circular maria are delineated. The majority of polygonal crater rims, linear portions of central peaks, crater chains, and certain linear mare ridges are related to the lineament systems. Spatial relationships of the lineament systems and other data indicate that the global systems resulted from compressive stresses in the moon's crust which were oriented in a north-south direction. Possible causes of these stresses are (1) the gradual subsidence of the "tidal bulge," (2) expansion and contraction of the moon, (3) lunar body tides, (4) convection currents within the moon as postulated by Runcorn, and (5) a shift of the moon's axis of rotation.

1. Introduction

Approximately 10,000 linear structures have been mapped within 60° of the moon's center of face. For each of 41 fields of the Photographic Lunar Atlas (1960), covering the 60° area, the most suitable sheets were selected as a base for mapping the lineaments. Each base photograph was supplemented by 5–10 photographs exhibiting various angles of illumination in order to aid in the identification of linear structures. The lineaments were checked and verified with almost 100 percent agreement, by W. K. Hartmann and E. A. Whitaker. This procedure eliminated personal bias regarding overall patterns, because the lineaments were first mapped from photographs of small areas prior to being replotted on a larger base map. Hence, there was no way of knowing whether or not a particular lineament trend would carry over into another area. In fact, a general pattern was not discernible until all the lineaments had been plotted on the large base map.

The mapped region encompassed by the 60° longitude and 64° latitude lines, was divided into four quadrants, each containing 85 areas of 33,464 sq km each. Lineaments within the areas were numbered and tabulated according to morphology (valley, ridge, rille, etc.) and degree of prominence

(very strong, strong, moderately strong, and weak). The end coordinates of each lineament were recorded and their length, true selenographic azimuth, and apparent azimuth, as seen in orthographic projection, have been computed on the IBM 7072 computer of the University of Arizona Numerical Analysis Laboratory. A statistical analysis of lunar lineaments and a comparison between lunar and terrestrial lineament patterns will be presented in a later *Communication*.

Lineaments mapped from the base photographs were replotted on the *USAF Lunar Reference Mosaic LEM-1*. It was possible to replot only about 80 percent of the lineaments since the quality of the Reference Mosaic was not adequate for identification of very small or relatively weak structures. Eight maps showing the lineament trends have been constructed and are listed below in Table 1. Maps 1A and 1B are to a scale of 1:3,800,000. All other maps have a scale of 1:5,700,000.

2. Lunar Lineaments

The *Dictionary of Geologic Terms* (1957) defines lineaments as: "(1) Significant lines of landscapes which reveal the hidden architecture of the rock basement. They are character lines of the earth's physiognomy. (2) An essentially rectilinear

TABLE 1

MAP	TITLE
1A-1B.....	Tectonic Map of the Moon
2.....	Radial Lineament Systems of the Moon
3.....	NW-SE Lunar Lineament System (Astronautical Directions) *
4.....	NE-SW Lunar Lineament System (Astronautical Directions)
5.....	N-S Lunar Lineament System (Astronautical Directions)
6.....	NNE-SSW Lunar Lineament System (Astronautical Directions)
7.....	Composite Map of the NW-SE, NE-SW and N-S Lunar Lineament Systems (Astronautical Directions)
8.....	Lunar Lineaments Unrelated to Major Systems

*Selenographic directions follow the convention adopted by the I. A. U. at Berkeley in 1961. North is at the top, while east is to the right and west is to the left.

topographic feature resulting from a fault. (3) A topographic line that is structurally controlled." These descriptions are applied to terrestrial lineaments, but may also be used to define linear structures on the moon. One further restriction is applied to lunar lineaments in this paper: since the features must be relatively linear in structure, arcuate features such as the Liebig fault, the Hippalus rilles, and concentric scarps are not classified as lineaments, although some of these features are shown on Maps 1A and 1B. This also applies to very sinuous mare ridges.

Lunar lineaments have been classified into eight morphological types: (a) ridges on terrae, (b) valleys, (c) polygonal crater rims, (d) definite linear faults, (e) crater chains, (f) linear rilles, (g) linear ridges in the maria, and (h) linear portions of central peaks.

(a) As their names imply, ridges on terrae are positive features occurring primarily in the uplands, while valleys are negative structures. Terrae ridges consist of upland material and do not usually exhibit any well-defined crustal displacement.

(b) Valleys are primarily associated with radial systems, although they are not necessarily restricted to these systems. A majority of valleys are related to the Imbrium radial system. They are probably graben with considerable vertical displacement, or fissures due to horizontal cracking of the crust. A number of features which are depicted as valleys may actually be series of coalescing craters. These features have engrailed walls but the photographic resolution is not sufficient for true crater-form outlines to be distinguished.

(c) Linear crater rims are classified as lineaments. They consist of the crest of the rim only, and do not include interior terracing, exterior linear structures on crater slopes, or the dissected crater rims which occur primarily in the Sinus Medii-Mare Vaporum region.

(d) Only those features which show definite displacement of the surface are classified as faults. These are mostly young, well-defined structures, e.g., the Straight Wall, and are probably normal faults. Many of the ridges may be faults also, but in most cases there is little or no indication of the type of movement which may have occurred.

(e) A series of craters is considered to be a crater chain if it consists of three or more evenly spaced craters lying along a straight line. Usually the craters forming the chain are similar in degree of sharpness and often have similar diameters, or a progressive decrease in diameter. Crater chains are depicted as rows of circles on the maps. However, neither the number of circles nor their diameters necessarily represent the true number or diameter of craters in any individual chain.

(f) Rilles can be classified into four types according to their geometry: (1) linear, (2) arcuate, (3) irregular, and (4) sinuous. Linear rilles, e.g., Ariadaeus rille, are straight and occur anywhere in marial areas, while arcuate rilles, e.g., the Hippalus rilles, are gently curved features which occur along the margins of maria or in the lava-filled interiors of craters. Irregular rilles, such as the Triesnecker and Littrow systems, are groups of branching, bifurcated rilles which are probably due to complex local forces. The sinuous rilles, e.g., the Marius, Hadley, and Conon rilles, are winding features having the appearance of meandering river beds. This type of rille generally starts at a small crater and may have an entirely different (nontectonic) origin than the other types of rilles. Schröter's Valley is a conspicuous example of this type of feature. In accordance with our definition of the term, only the linear type of rille is classified as a lineament.

(g) Mare ridges are classified as lineaments if they are straight. They usually occur in groups and often *en échelon*, as do the short mare ridges southwest of the Straight Wall. In some instances long mare ridges are broken up into linear segments, as in the Serpentine Ridge.

(h) Linear portions of central peaks in craters have the same morphology as terrae ridges and valleys. However, they may comprise either the entire central peak or small portions of the peak.

3. Tectonic Maps

(a) Tectonic Map of the Moon. (Map 1A, 1B)

This map is in two halves which may be assembled by cutting along the medianal olive line on Map 1A and matching it to the north and south fiducial marks of Map 1B. All lineaments are shown on this map, together with the most prominent mare ridges and rilles.

(b) Radial Lineament Systems of the Moon.

Map 2 shows radial lineament systems associated with (1) Mare Imbrium (black), (2) Mare Nectaris (red), (3) Mare Humorum (blue), and (4) Mare Crisium (green). The system surrounding Mare Crisium is incomplete because the eastern portion is outside the area of investigation. Similarly, the radial systems associated with Mare Orientale and Mare Humboldtianum are not shown (See *Comm.* No. 36).

Map 2 was drawn by constructing great circles radial to the circular maria and plotting the lineaments approximately parallel to these lines. Actually, the radial systems do not converge to a point source, but radiate from a circle-of-confusion coincident with the diameter of the inner basins.

An examination of the map reveals that there are east-west gaps in all radial patterns. Hartmann (1963, 1964), who has studied the radial systems in detail from rectified photographs, also reports gaps in the radial patterns east of Mare Orientale and Mare Crisium.

It might appear that the east-west gaps are due to observational error resulting from the difficulty of recognizing lineaments which parallel the sun's rays and therefore cast little or no shadow. However, this zone would be restricted to angles of about 5–10° to the north and south of latitude lines. With the exception of the western gap of Mare Nectaris and the east and west gaps of Mare Imbrium, all gaps are of the order of 80–90°. The east and west gaps of Mare Imbrium are about 30 and 50° respectively, while the western gap of Mare Nectaris is 45°. In addition, radial lineaments are relatively strong features and would be expected to show even under adverse lighting conditions. Also, if the gaps were due to poor visibility of lineaments parallel to the sun's rays, one would expect a gradual decrease in the apparent number of lineaments as an east-west orientation was approached. However, the transition from the radial pattern to the gaps is very abrupt, as is illustrated on Map 2. Therefore, it seems definite that the east-west gaps are structural breaks in the radial systems.

Another unique feature illustrated on Map 2 is that Mare Nectaris has two radial systems. The major system, represented by unbroken red lines, is centered on the inner basin, while a minor system (dashed red lines) is focused on the southern edge of the inner basin. The lineaments of both systems are of equal intensity, but the system centered near Fracastorius occurs only south of the mare. At first sight it might appear that the minor system is associated with Fracastorius rather than Mare Nectaris. However, it seems highly improbable that such a relatively small structure could cause such a strong radial system when craters the size of Janssen, Clavius, or Ptolemaeus are devoid of radial structures. Therefore, it seems certain that the secondary system is associated with Mare Nectaris and is contemporary with its formation. This minor system is also asymmetrically placed in regard to the concentric scarp system surrounding Mare Nectaris (See Hartmann and Kuiper, 1962). It seems probable that two sets of stresses were superposed in such a way as to produce two contemporaneous radial structures.

Mention should be made of the two prominent zones of radial lineaments to the southwest of Mare Nectaris and to the southeast of Mare Humorum. These zones are very pronounced because they coincide with the directions of the global NW-SE and NE-SW lineament systems. It is therefore impossible to determine which lineaments should be classed with the radial systems and which should be placed with the global systems. It is probable that the lineaments in these zones belong to both the radial and global systems.

From a detailed study of the radial systems, Hartmann (1963, 1964) has concluded that the structures radial to circular maria are caused by tectonic activity rather than being grooves produced by secondary ejecta. The writer agrees with this interpretation for the reasons given by Hartmann. Furthermore, it seems impossible to explain the existence either of two radial systems associated with one mare, or of the east-west gaps in radial patterns by the hypothesis of secondary ejecta. Also, the fact that the morphology of many radial lineaments is identical to that of the global systems, which are definitely the result of tectonic activity, appears incompatible with the secondary ejecta hypothesis. The radial lineament systems are probably tension fractures and graben which have resulted from tensile stresses concentrically oriented around the mare basins, and probably caused by the

gentle doming of a vast area surrounding the basins.

(c) *Global Nonradial Lineament Systems.* Maps 3–6 depict four global nonradial lineament systems. The directions given in the titles of Maps 3, 4, and 6 refer to the orthographic tangential plane and are approximate to selenocentric directions.

Azimuth-frequency diagrams of the lineaments have been constructed for various parts of the lunar surface, and were used as one basis for delineating the four nonradial lineament systems. Figures 1 and 2 are diagrams of the frequency of *apparent* azimuths in orthographic projection of lineaments which occur in portions of the moon's northern and southern hemispheres. The diagrams represent areas relatively free from radial lineaments and show the four principal directions of the global systems. Figure 1 also displays a strong peak formed by the Imbrium radial system. Figure 2 does not show the Imbrium radial system because (1) the Imbrium lineaments form a relatively uniform fan-shaped pattern in this area, (2) many of the Imbrium lineaments coincide with the directions of the nonradial systems, and (3) the density of the Imbrium lineaments in this area is much less than the density of the nonradial lineaments. The azimuth-frequency diagrams should be studied in conjunction with Maps 1A and 1B in order to visualize the spatial relations of the lineaments.

Fielder (1963) has investigated lunar lineaments and also delineated four global lineament systems. His "A," "B," and "C" systems of lineaments correspond to the author's NW-SE, NE-SW and N-S lineament systems. He also found limited evidence for an E-W lineament system (system "D") which I was unable to detect. I have been able to detect a weak NNE lineament system which Fielder (personal communication) has recognized in subsequent investigations. The correspondence in directions and spatial relations between our lineament systems is remarkable considering that the investigations were completely independent.

(d) *NW-SE and NE-SW Lunar Lineament Systems.* Maps 3 and 4 are a compilation of lineaments belonging to the NW-SE and NE-SW systems. These systems are approximately orthogonal and nearly coincide with the trend of small circles. Therefore, the lineaments are approximately parallel when viewed in orthographic projection. Actually, the systems are more nearly barrel-shaped as stated by Fielder (1963) and correspond to his systems "A" and "B." The poles of these systems are situated about 45–55° to the east and west of the moon's

axis of rotation. Figures 3 and 4 are globe projections of the NW-SE and NE-SW systems as seen from directly over their southwestern and southeastern poles, respectively. They clearly show the small-circle trend of the lineaments, although the barrel shape of the systems has produced a very slight flattening of the small circles. Both systems have a paucity of lineaments in the limb regions of their equatorial planes.

Linear mare ridges in Mare Frigoris, Mare Nubium, and Oceanus Procellarum, as well as the Abulfeda crater chain and the major axes of Schiller and Rheita E, coincide with the directions of these systems.

(e) *N-S Lunar Lineament System.* The N-S system nearly lies on great circles approximately parallel to the meridians. Actually the north-south lineaments slightly deviate from the meridians so that they converge on the area encompassed by the 75° latitude. The poles of this system are the same as the moon's axis of rotation. Fielder (1963) has mapped this system which he denotes as system "C." However, he finds that the lineaments lie on small circles. If he has placed some of the radial lineaments south of Mare Humorum and Mare Nectaris in this system, this would make them appear to lie on small circles. Also, Fielder (personal communication), has mapped the N-S system only within 40° of the center of face. When the mapped lineaments are extended to 60° from the center of face it is obvious that those associated with the N-S system are approximately parallel to meridians (See Fig. 5). There are small groups of parallel lineaments in the Taurus Mountains region and southeast of Mare Humorum which deviate from the meridional directions and would coincide with Fielder's north-south small-circle system (See Map 8). However, the dominant trend in these regions is nearly along the meridians, and therefore the author does not feel that the small groups of lineaments which deviate from this trend are sufficiently numerous to justify their inclusion into a separate system.

(f) *NNE-SSW Lunar Lineament System.* The NNE-SSW system is less well developed than the other major systems. The lineaments of this system lie on small circles whose planes are at angles of about 15–20° to the moon's axis of rotation. It is difficult to determine the aerial distribution of this system because great-circle N-S lineaments coincide with the direction of NNE-SSW small-circle lineaments in the southeast limb region. There is probably an intermingling of the two systems in this area.

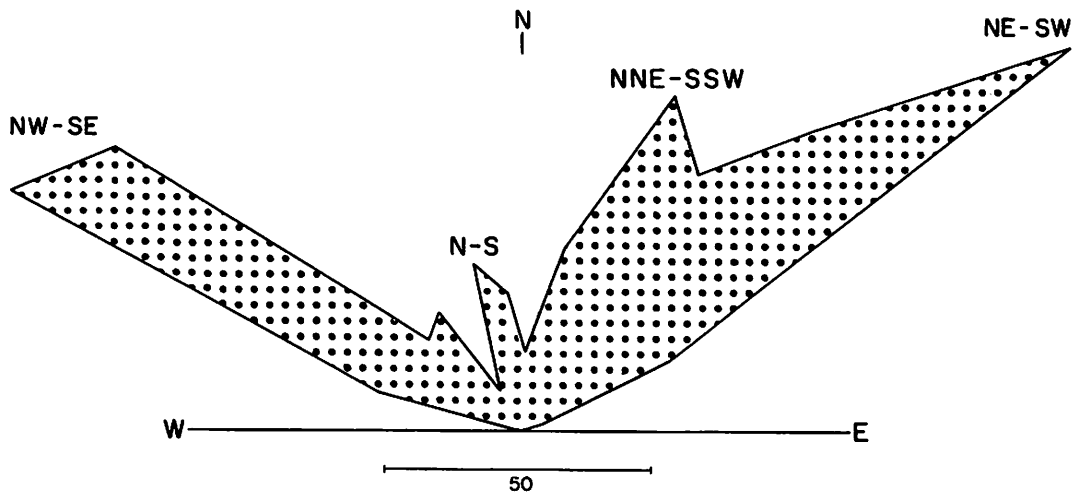
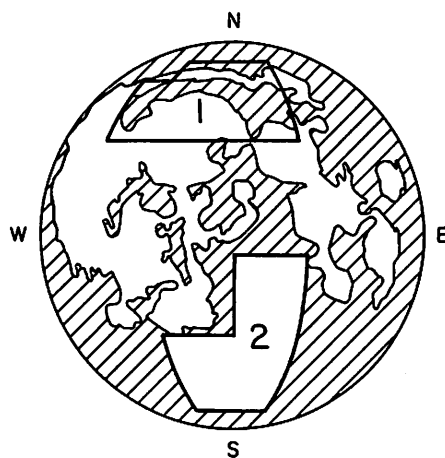


Fig. 1. Azimuth-frequency diagram of lineaments in a portion of the moon's northern hemisphere. The diagram represents the apparent azimuths as viewed in orthographic projection.



(Key to areas shown in Figs. 1 and 2.)

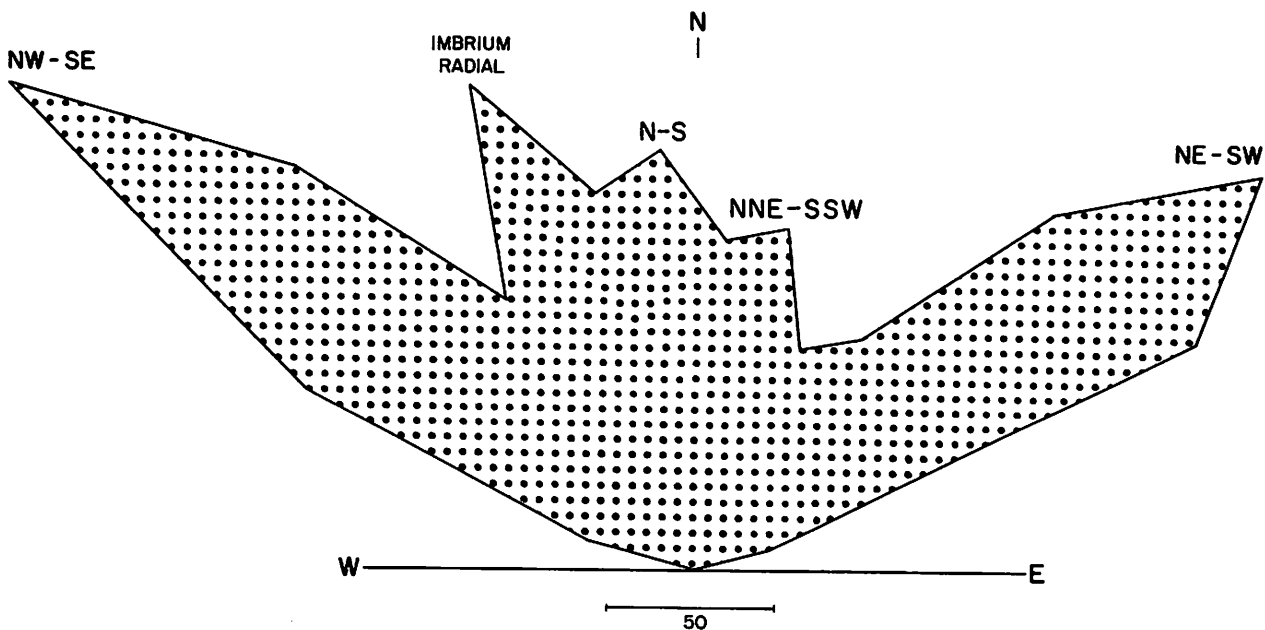


Fig. 2. Azimuth-frequency diagram of lineaments in a portion of the moon's southern hemisphere. The diagram represents the apparent azimuths as viewed in the orthographic projection.

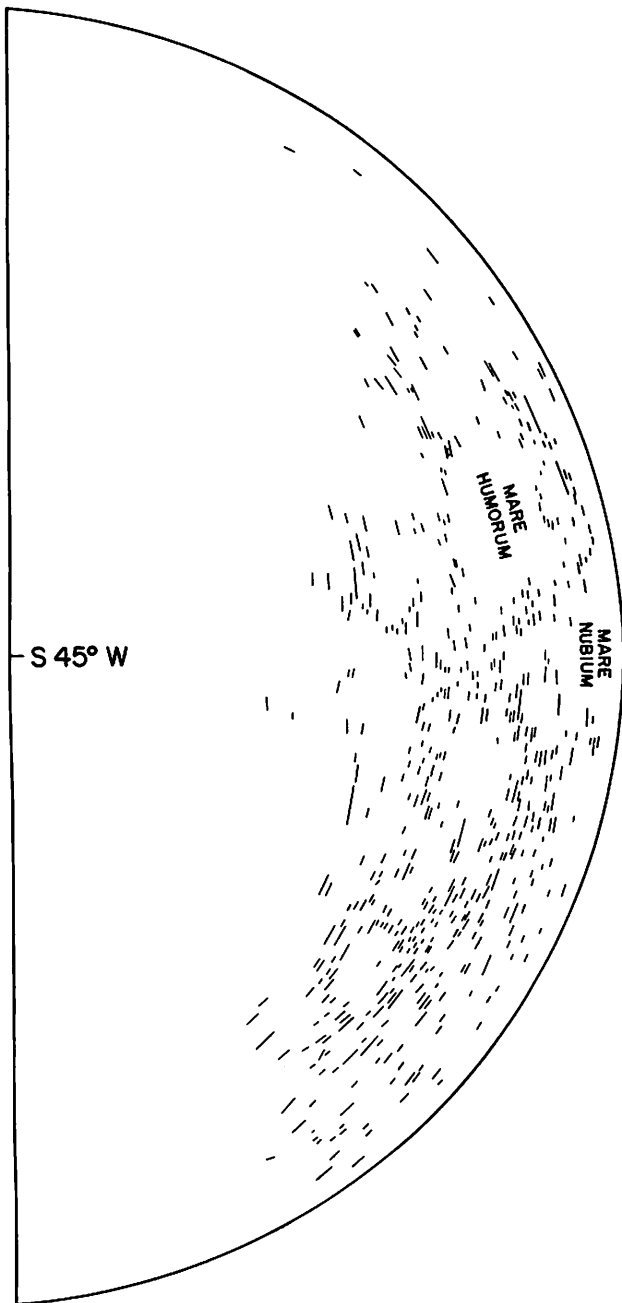


Fig. 3. Globe projection (tracing) of the NW-SE lineament system as seen from directly over its southwestern pole.

This observational difficulty accounts for the lack of NNE-SSW lineaments shown in the southeastern limb region of Map 6.

(g) *Composite Map of the NW-SE, NE-SW, and N-S Lunar Lineament Systems.* Map 7 is a composite of the three major nonradial lineament systems, and illustrates their spatial relationships. In the orthographic plane, the axes of symmetry of the NW-SE and NE-SW systems are lines situated

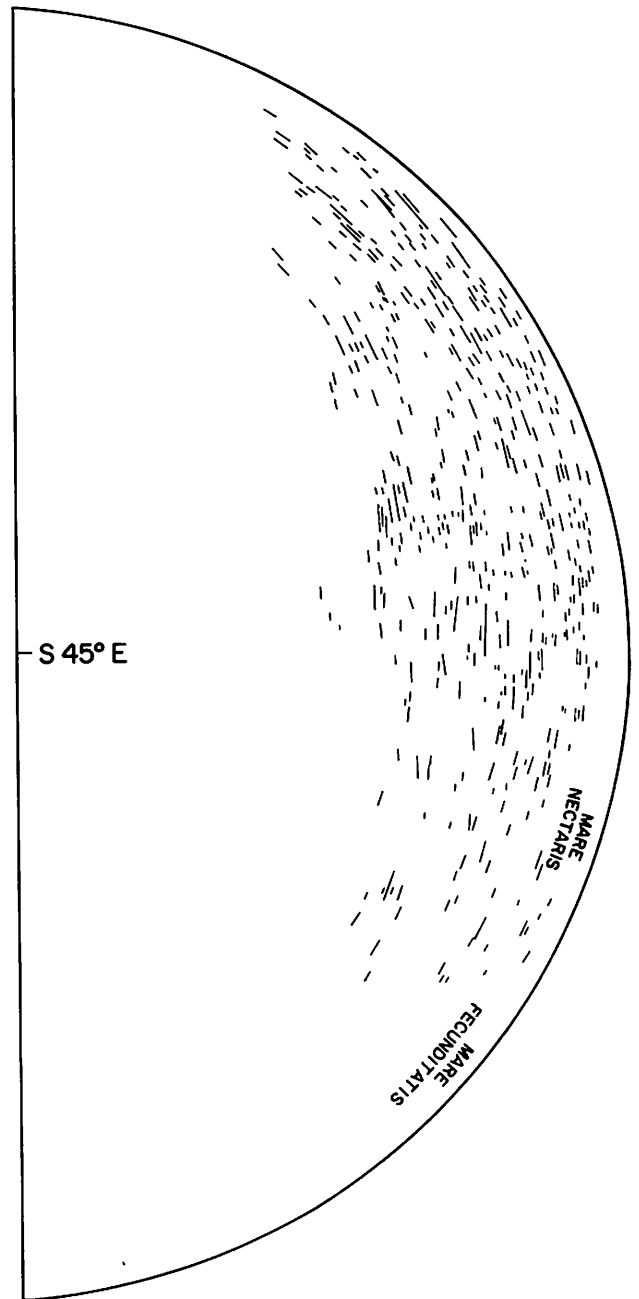


Fig. 4. Globe projection (tracing) of the NE-SW lineament system as seen from directly over its southeastern pole.

approximately $45\text{--}55^\circ$ to the east and west of the moon's axis of rotation. The angles of intersection of these systems vary from $90\text{--}120^\circ$ as seen in orthographic projection.

(h) *Lunar Lineaments Unrelated to Major Systems.* Map 8 is a compilation of all lineaments which do not belong to the major global or radial systems. A comparison of this map with Maps 1A and 1B demonstrates that no more than five percent of the

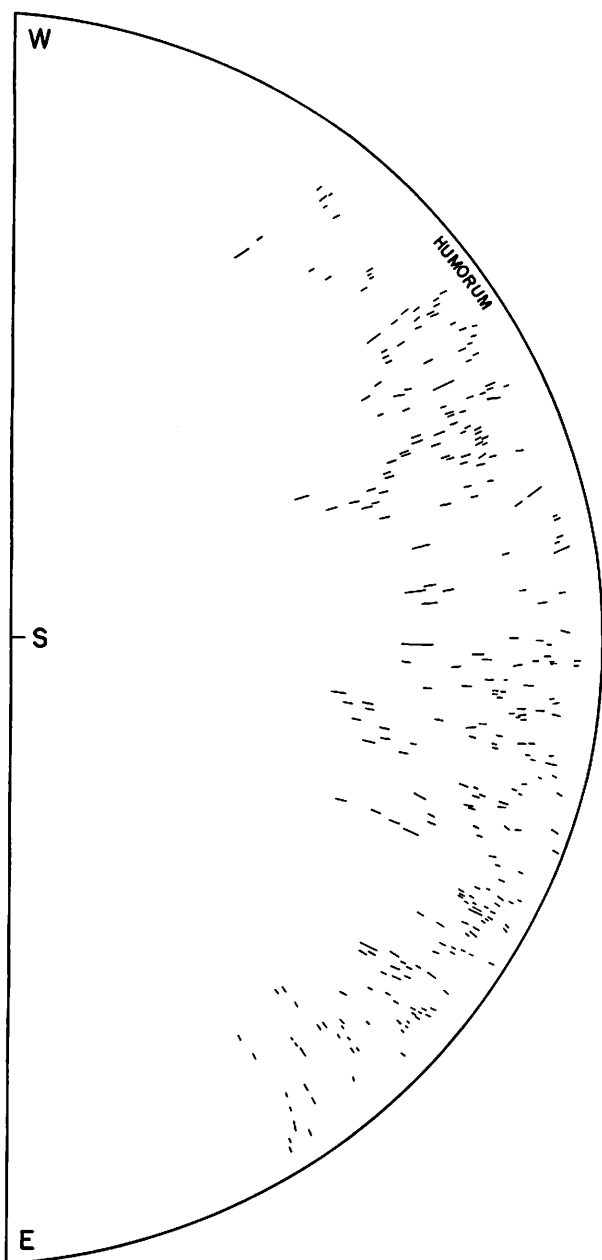


Fig. 5. Globe projection (tracing) of the N-S lineament system as seen from directly over its southern pole.

lineaments are unrelated to the radial or nonradial systems. Nevertheless, many of these occur as groups of parallel lineaments which present fairly extensive trends, such as the NNW-SSE trending lineaments in the vicinity of Mare Nubium. The lineaments depicted on Map 8 are probably fractures which have resulted from local stresses induced by the primary stresses which formed the major lineament systems.

4. Morphological Relationships

A preliminary count of the number of different types of lineaments which occur in the various lineament systems is shown in Table 2. The count is not complete since about 20 percent of the lineaments could not be replotted on the larger base map. However, the sample is large enough to insure that the statistical relationships will hold when the remaining lineaments have been classified.

Of a total of 362 polygonal crater rims, 94 percent coincide with the directions of the radial and nonradial systems. Eighty-three percent of the total are coincident with the directions of the four nonradial systems. Only six percent are unrelated to either the radial or global systems. It seems evident from these figures that polygonal crater rims are related to the lineament systems, particularly to the nonradial systems. The polygonal outline of craters is undoubtedly due to the fracture patterns which governed their shape along pre-existing zones of weakness associated with major lineament trends. Many terrestrial calderas, explosion craters, and impact craters exhibit similar polygonal rims. It has been demonstrated that these polygonal rims are the result of pre-existing joint or fracture patterns. Fullmer and Roberts (1963) have studied explosion craters and found "that the parent joint fabric of the rock medium is an important controlling factor, influencing crater shape and the character of the larger ejected fragments." Darling (1948) has observed similar conditions during cratering tests in basalt. He states, "The hardness of the material and the varying joint conditions of basalt contribute greatly to the fluctuations. It can be seen that original horizontal and vertical jointing affected the shape and size of the craters." Meteor Crater, Arizona, is a terrestrial impact crater which also exhibits a polygonal shape. The crater is roughly rectangular in outline, and its shape has been controlled by regional jointing (Shoemaker, 1959).

A total of 43 crater chains has been mapped. Eighty-seven percent of these features coincide with the directions of the radial and nonradial lineament systems. Sixty-nine percent are associated with the four nonradial systems only, and 13 percent are unrelated to any system. These figures suggest that the majority of crater chains are volcanic craters which have arisen along fractures associated with the major lineament systems.

A similar case exists for the linear portions of central peaks. The azimuths of 92 percent of these features, out of a total of 58, correspond to the direc-

tions of the radial and nonradial systems. Seventy percent coincide with the four directions of the nonradial systems, while only eight percent are unrelated to either the radial or nonradial systems. Here, again, is a strong relationship between the central peaks which exhibit linear structures and the major lineament systems. It would appear that the majority of central peaks exhibiting linear structures have risen along fractures associated with the major lineament systems, or, at least, their configuration has been influenced by the regional fracture patterns.

Nectaris, (4) Crisium, (5) Humorum, (6) Humboldtianum.

(b) Mare Nectaris possesses two radial systems. The major system is focused on the inner basin. A minor system is south of the mare only and is centered on the southern edge of the inner basin.

(c) All radial systems have an east-west structural gap in their radial pattern. With the exception of the Imbrium system and the western portion of the Nectaris system, the magnitudes of the gaps are generally 80–90°.

TABLE 2.
MORPHOLOGICAL RELATIONSHIPS

LINEAMENT SYSTEMS	NUMBER OF POLYGONAL CRATER RIMS		NUMBER OF LINEAR CENTRAL PEAKS		NUMBER OF CRATER CHAINS	
	UNDIFFERENTIATED*	RADIAL ONLY	UNDIFFERENTIATED*	RADIAL ONLY	UNDIFFERENTIATED*	RADIAL ONLY
<i>Radial</i>						
Imbrium	37	31	9	8	8	7
Nectaris	23	5	9	4	3	1
Humorum	17	0	4	1	1	0
Crisium	13	5	0	0	0	0
Totals	90	41 (11%)	22	13 (22%)	12	8 (18%)
<i>Nonradial</i>						
NW-SE	108		12		8	
NE-SW	127		7		8	
N-S	53		20		5	
NNE-SSW	13		2		9	
Totals	301 (83%)		41 (70%)		30 (69%)	
<i>Unrelated</i>	20 (6%)		4 (8%)		5 (13%)	
Totals	362		58		43	

*Lineaments coincident with both radial and nonradial systems.

As previously mentioned, the azimuths of certain groups of linear mare ridges conform to the directions of the major lineament systems (see Pls. 1a, 1b, 2a, and 2b). The similarity in spatial relationships of the terrae lineaments and the linear mare ridges is too striking to be fortuitous. These linear ridges in the maria have probably resulted from the same stresses which gave rise to the terrae lineaments, indicating that the stresses which produced the lineament patterns were still active — but considerably reduced in magnitude — after the mare flooding had occurred. This should not be interpreted as meaning that *all* mare ridges have resulted from these same forces; they definitely have not. Most of the mare ridges are very sinuous and form a concentric pattern which follows the outline of the mare basin. These concentric mare ridges probably resulted from local forces within the basins.

5. Summary and Conclusions

(a) Radial lineament systems are associated with six circular basins; listed in decreasing order of intensity they are: (1) Imbrium, (2) Orientale, (3)

(d) There are four global nonradial systems: (1) NW-SE, (2) NE-SW, (3) N-S, (4) NNE-SSW.

(e) The global systems cross the moon's surface in well-defined directions for thousands of kilometers.

(f) The N-S system nearly lies on great circles and roughly parallels the meridians.

(g) The lineaments of the NE-SW and NW-SE systems nearly coincide with the trend of small circles and therefore are approximately parallel when viewed in orthographic projection.

(h) In the orthographic plane, the axes of symmetry of the NW-SE and NE-SW system are lines situated approximately 45–55° to the east and west of the moon's axis of rotation.

(i) The angles of intersection of the NE-SW and NW-SE systems vary from 90–120°, as seen in orthographic projection.

(j) Both the NE-SW and NW-SE systems contain few lineaments in the limb regions of their equatorial plane.

(k) The majority of polygonal crater rims, linear portions of central peaks, crater chains, and certain

linear mare ridges are preferentially oriented in the same directions as the radial and nonradial lineament systems.

The lineaments of the global nonradial systems cross the moon's surface in well-defined directions for thousands of kilometers, indicating that the forces which produced them were relatively uniform in magnitude and direction (as Anderson, 1951, found for the earth), and affected the entire crust of the moon. This essentially eliminates large meteorite impacts as a source of the stresses which caused the nonradial systems, although minor deviations in the directions of the systems may have resulted from such stresses. It seems conclusive that lunar lineaments are fractures or zones of weakness which were internally produced by tectonic activity.

The genesis of the nonradial lineament systems can be readily explained by compressive stresses in the moon's crust which have acted in a north-south direction (see Fig. 6). It is well known from geo-

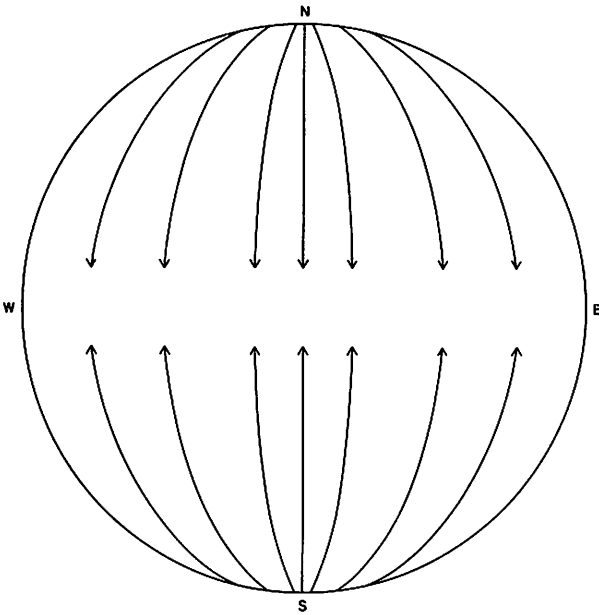


Fig. 6. Probable orientation of crustal stresses which produced the nonradial lineament systems.

logical studies that a principal compressive stress acting in the horizontal plane will produce planes of maximum shearing stress which lie at angles of about 45° on either side of the axis of maximum compression (Billings, 1954; de Sitter, 1956). The planes of actual shear do not necessarily coincide with the planes of maximum shearing stress but may be lo-

cated at angles of $30\text{--}55^\circ$ from the axis of maximum compression. Physical properties of the material and the orientation of the principal stresses are factors which contribute to the deviation in direction between the actual shear and the theoretical maximum stress. Tension fractures will develop at right angles to the least principal stress axis which is perpendicular to the axis of maximum compression (see Fig. 7). Under these considerations the NW-SE and NE-SW lineament systems are probably shear fractures which have formed at angles of $45\text{--}55^\circ$ from

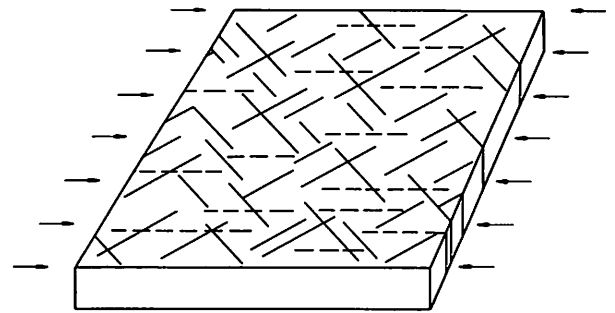


Fig. 7. Shear (unbroken lines) and tension (broken lines) fractures produced by horizontal compression.

north-south axes of maximum compression, and the N-S lineament system consists of tension fractures parallel to these axes.

If this theory is correct then the bisectors of the angles made by the NW-SE and NE-SW systems will be oriented along the directions of the axes of maximum compression and should parallel the directions of the N-S system. Figure 8 is a diagram of the three major nonradial systems as seen from directly above the moon's south pole. The diagram was constructed by projecting the composite lineament map (Map 7) onto a globe and photographing it from directly over the south pole. The lineament directions of each system were smoothed and the bisectors of the angles made by the orthogonal systems (NW-SE and NE-SW) were constructed. The bisectors are represented by arrows in Figure 8 and point to the angles they bisect. They may also be regarded as the axes of maximum compression. It is apparent that the bisectors radiate from the south polar region and nearly parallel the north-south lineament directions. These orientations of the maximum stress axes account for the small-circle trend of the NW-SE and NE-SW lineament systems.

The NNE-SSW lineament system probably consists of second-order shear fractures which have

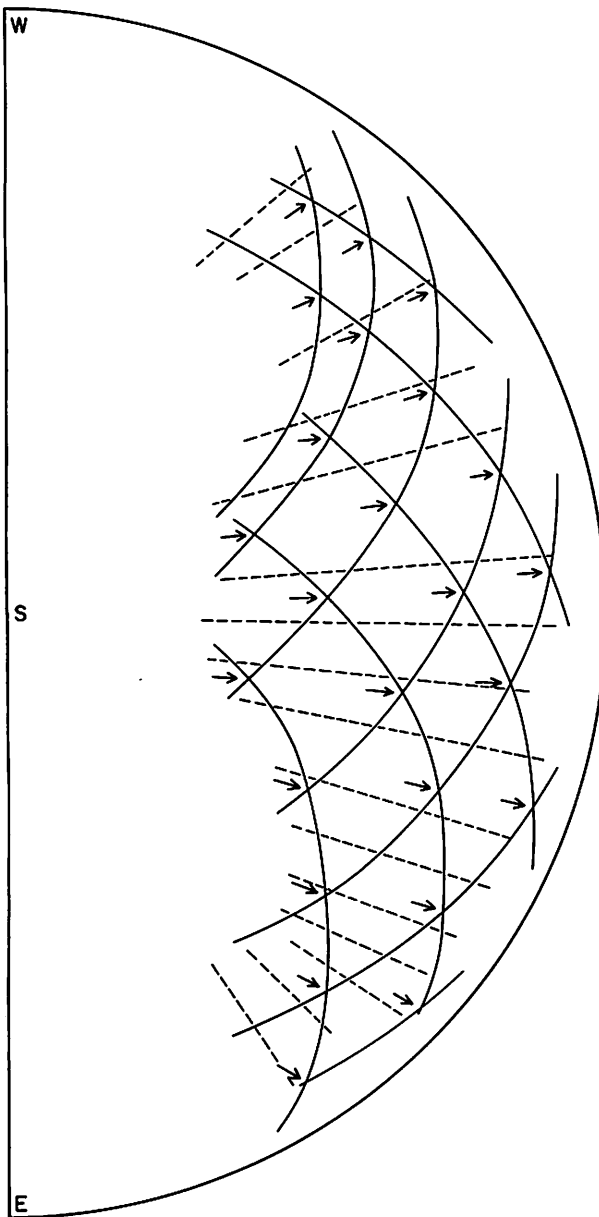


Fig. 8. South polar projection of the lineament systems, showing the smoothed directions of the NW-SE, NE-SW and N-S (dashed lines) systems. The arrows are bisectors of angles formed by the NW-SE and NE-SW systems. They may also be regarded as axes of maximum compression.

resulted from local reorientation of compressive stresses due to inertial, frictional, or body forces involved during movement on the primary shear planes. Second-order features of this nature often accompany primary shear fractures on earth and usually form at angles of $15\text{--}30^\circ$ from the primary shear direction (Moody and Hill, 1956). The NNE-SSW system intersects the NE-SW system at angles of about 30° . One would expect a complementary

second-order shear system associated with the NW-SE system. Previous mention was made of a weak NNW-SSE group of lineaments shown on Map 8 in the vicinity of Mare Nubium. This set of lineaments may represent a very weak second-order shear system associated with the primary NW-SE system.

According to theory one might expect a major lineament system consisting of compression fractures or thrust faults which are oriented at right-angles to the axis of maximum compressive stress, or in an east-west direction. However, no east-west lineament system could be found. There are several widely dispersed lineaments oriented in an east-west direction but these are too infrequent and widely disseminated to warrant their inclusion into a lineament system. Three possible explanations may account for the apparent lack of an east-west system. As previously mentioned, east-west oriented lineaments would be difficult to recognize because they parallel the sun's rays and therefore cast little or no shadow. Secondly, these lineaments would presumably consist of compression fractures or thrust faults, and whenever there is a fault scarp marking the edge of a thrust sheet, it is likely to be less imposing and more sinuous and irregular in plan than one associated with a wrench or normal fault. Therefore, this type of feature would be much more difficult to recognize than shear or tension fractures. A third possibility is that compression fractures did not form. It is known from laboratory experiments that compression fractures are usually the last type of fault to form, because the compressive strength of rocks is greater than either their tensile or shearing strengths. Hence, it is possible that all or most of the stresses were dissipated during the formation of the tension and primary and second-order shear fractures. Any remaining stresses may have been insufficient to form thrust faults.

The east-west structural gaps in radial systems are additional evidence strongly suggesting a global north-south compression. As previously stated, the radial systems have probably resulted from tensile stresses concentrically oriented around the mare basins. East and west of the basins this tensile stress would have acted in a north-south direction. However, a north-south oriented compression would counteract the north-south tension and produce a zone of no stress to the east and west of the basins. Therefore, no radial lineaments would form in these regions. The Imbrium system probably has smaller east-west gaps ($30\text{--}50^\circ$) because the forces which formed the system were obviously far greater than

the forces that formed the other radial systems and were able to overcome the north-south compression to a greater degree.

There have been many statements in the literature about the apparent absence of strike-slip movement on the moon. Most of these statements cite the absence of horizontal displacement of crater rims as evidence against wrench faulting. However, Fielder (1963, 1964) has found evidence for strike-slip faulting based on small displacements of crater rims and elliptical craters in the Mare Vaporum region. He cites evidence of horizontal movement along the Capella Fault, Deslandres-Regiomontanus fault, the Alpine Valley, and the Abulfeda crater chain. The amount of offset ranges from maximums of 10–32 km. Also the northern rim of Clavius may be offset as much as 30 km. The sense of movement along these faults is consistent with a medianal compressive stress in the moon's crust, e.g., right-lateral movement along the NW-SE faults and left-lateral movement along the NE-SW faults.

This isolated evidence for strike-slip movement is still not strong enough to definitely prove that extensive wrench faulting has occurred on the moon. The vast majority of lineaments give no indication of the type of movement which may have occurred. However, the faults along which Fielder has found evidence of horizontal displacement are all very long (220–360 km). The majority of lineaments are short (5–40 km), and would be expected to have horizontal offsets of no more than a few kilometers. Such small offsets could hardly be recognized from earth-based photography. If such small offsets occurred on these lineaments the cumulative amount of horizontal displacement would be thousands of kilometers. This may be one reason why there are no major wrench faults comparable to the San Andreas or Great Glen faults. Small increments of strain would have been relieved along a great many small faults rather than great increments of strain being relieved along several large faults.

The north-south compressive stresses to which the moon's crust has been subjected were probably active primarily from the moon's beginnings through the formation of the maria, after which they gradually subsided to the present time. Recent observations of reddish spots near Aristarchus (Greenacre, 1963) and the Kosyrev (1962) observation of emissions from the central peak of Alphonsus may indicate slight present-day tectonic activity.

The primary problem is to establish a cause of the north-south compression. Fielder (1963) has

also concluded that the nonradial lineament systems are the result of a medianal pressure in the moon's crust and favors Runcorn's (1963) hypothesis of convection currents in the lunar mantle as the cause of this pressure. This hypothesis is attractive from a tectonic viewpoint because Runcorn's calculated distribution of horizontal velocity components (Fig. 9) would impart compressive stresses to the moon's crust which would act from the equator toward the north and south poles. However, we have seen that the spatial relationships of the lineaments

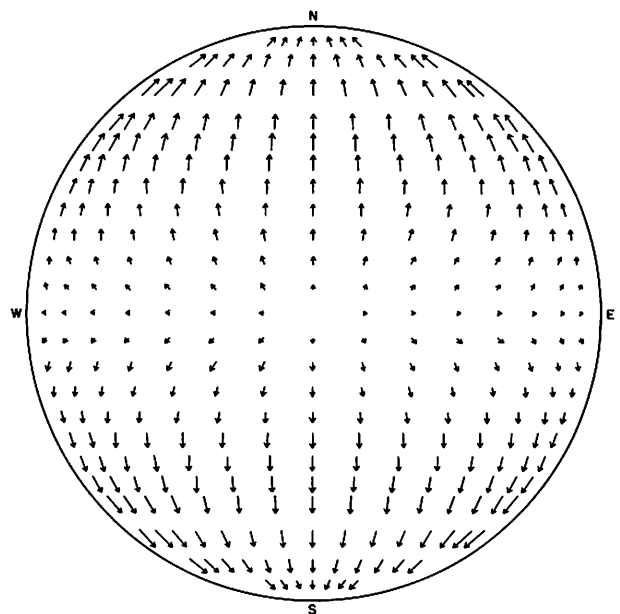


Fig. 9. Distribution of horizontal velocity components produced by Runcorn's hypothetical convection currents in the moon. Lengths of arrows are proportional to flow speeds. (After Runcorn with modifications.)

require the stresses to have been relatively uniform in magnitude and direction. Figure 9 shows that the stresses would be oriented in an east-west direction near the equatorial region and that the speed of the horizontal velocity components, and therefore the magnitude of the stresses, increases toward the north and south poles. This should produce a broad zone of tension in the equatorial region, but to date there is no surface evidence for such a zone of tension. The hypothesis of lunar convection currents is highly speculative and requires much further study before it can be accepted or rejected. This is especially true since terrestrial convection currents are as yet unproven.

Other possible causes of a north-south compression are (a) the gradual subsidence of the "tidal bulge" as the moon recedes from the earth, (b) expansion and contraction of the moon, (c) a change in the possible axis of flattening due to a shift of the moon's axis of rotation, and (d) lunar body tides due to librations in longitude and latitude, and the changing distance between the earth and moon. All of these factors may have played a part in producing the nonradial lineament systems of the moon. It remains for subsequent investigations to determine which factor was dominant.

Acknowledgments. The author wishes to thank Mr. Ewen Whitaker and Mr. William Hartmann for their verifications of lineaments and their many helpful suggestions. Mr. Paul Masser's help in programming lineament length and azimuth equations for the IBM 7072 computer is also gratefully acknowledged. The work reported here was supported by the National Aeronautics and Space Administration through Grant NsG 161-61.

REFERENCES

- Anderson, E. M. 1951, *The Dynamics of Faulting* (Edinburgh: Oliver and Boyd).
- Billings, M. P. 1954, *Structural Geology* (New York: Prentice-Hall, Inc.).
- Darling, James A. 1948, *Crater Tests in Basalt*. Dept. of Operations and Maintenance, Spec. Eng. Div. Panama Canal Zone, ICS Memo 284-P.
- de Sitter, L. U. 1956, *Structural Geology* (New York: McGraw-Hill.).
- Fielder, G. 1963 "Lunar Tectonics," *Quart. Jour. Geol. Soc. London*, 119, 65-94.
- . 1963, "Four Major Strike-Slip Faults on the Moon," *Geophys. Journ. of The Roy. Astron. Soc.*, 8, 2, 187-195.
- . 1964, "Strike-Slip Faulting in the Vaporum Region of the Moon," *Quart. Jour. Geol. Soc. London*, 120, 275-281.
- Fullmer, C. V. and Roberts, W. A. 1963, "Rock Induration and Crater Shape," *Icarus*, 2, 5-6, 452-465.
- Greenacre, J. A. 1963, "A Recent Observation of Lunar Color Phenomena," *Sky and Telescope*, 26, 6, 316-317.
- Haites, T. B. 1960, "Transcurrent Faults in Western Canada," *Journ. Alberta Soc. Petro. Geologists*, 8, 33-78.
- Hartmann, W. K. 1963, "Radial Structures Surrounding Lunar Basins, I: The Imbrium System," *Comm. L.P.L.*, 2, 24, 1-15.
- . 1964, "Radial Structures Surrounding Lunar Basins, II: Oriental and Other Systems; Conclusions," *Comm. L.P.L.*, 2, 36, 175.
- Hartmann, W. K. and Kuiper, G. P. 1962, "Concentric Structures Surrounding Lunar Basins," *Comm. L.P.L.*, 1, 12, pp. 51-66.
- Runcorn, S. K. 1963. *The Interior of the Moon*, Jet Propulsion Laboratory, Pasadena, TR 32-529.
- Shoemaker, E. M. 1959, *Impact Mechanics of Meteor Crater, Arizona*, Open File Report, U.S. Atomic Energy Comm.

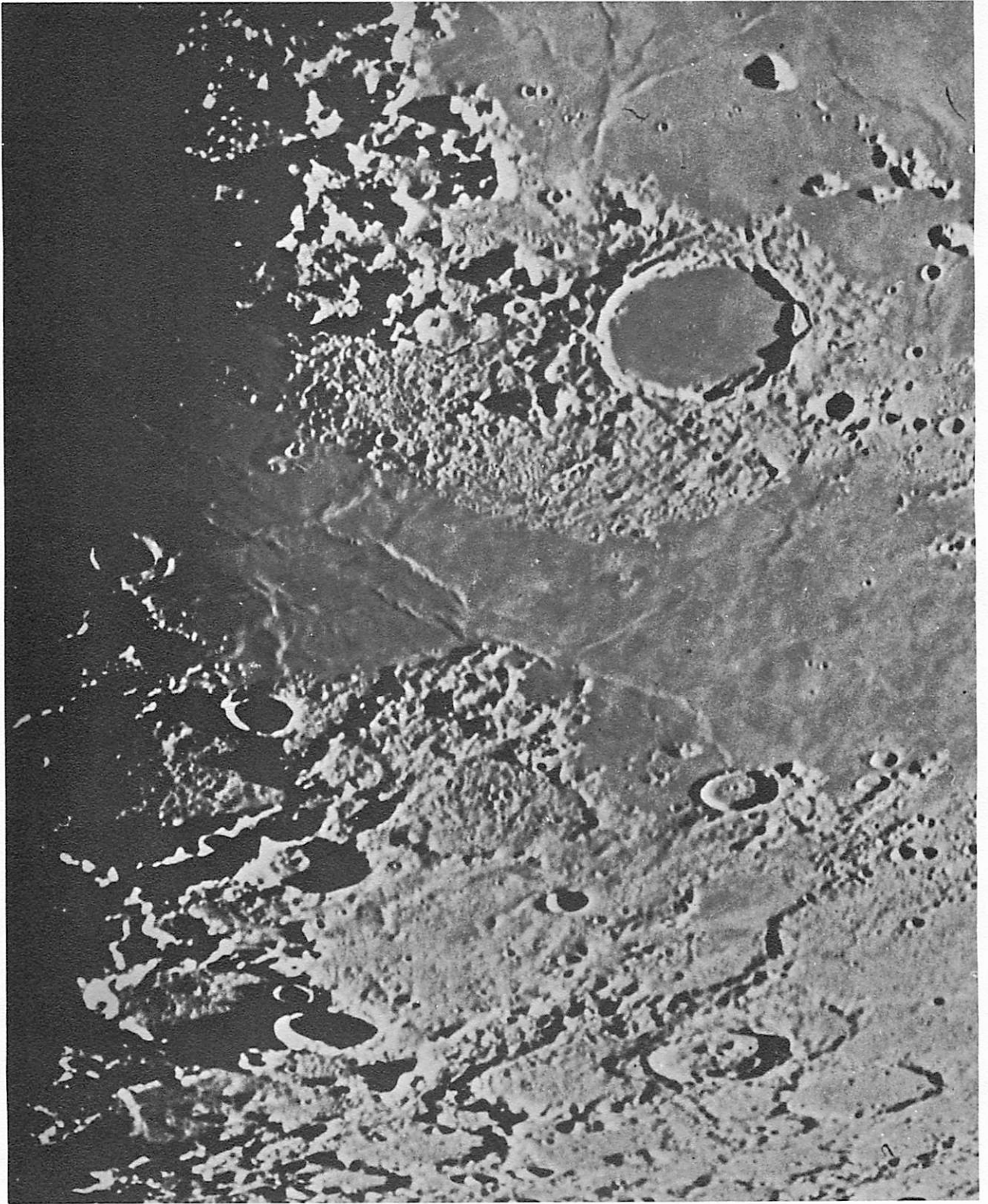


Plate 1a. Linear mare ridges in Mare Frigoris which coincide with the directions of lineaments in the adjacent terrae.

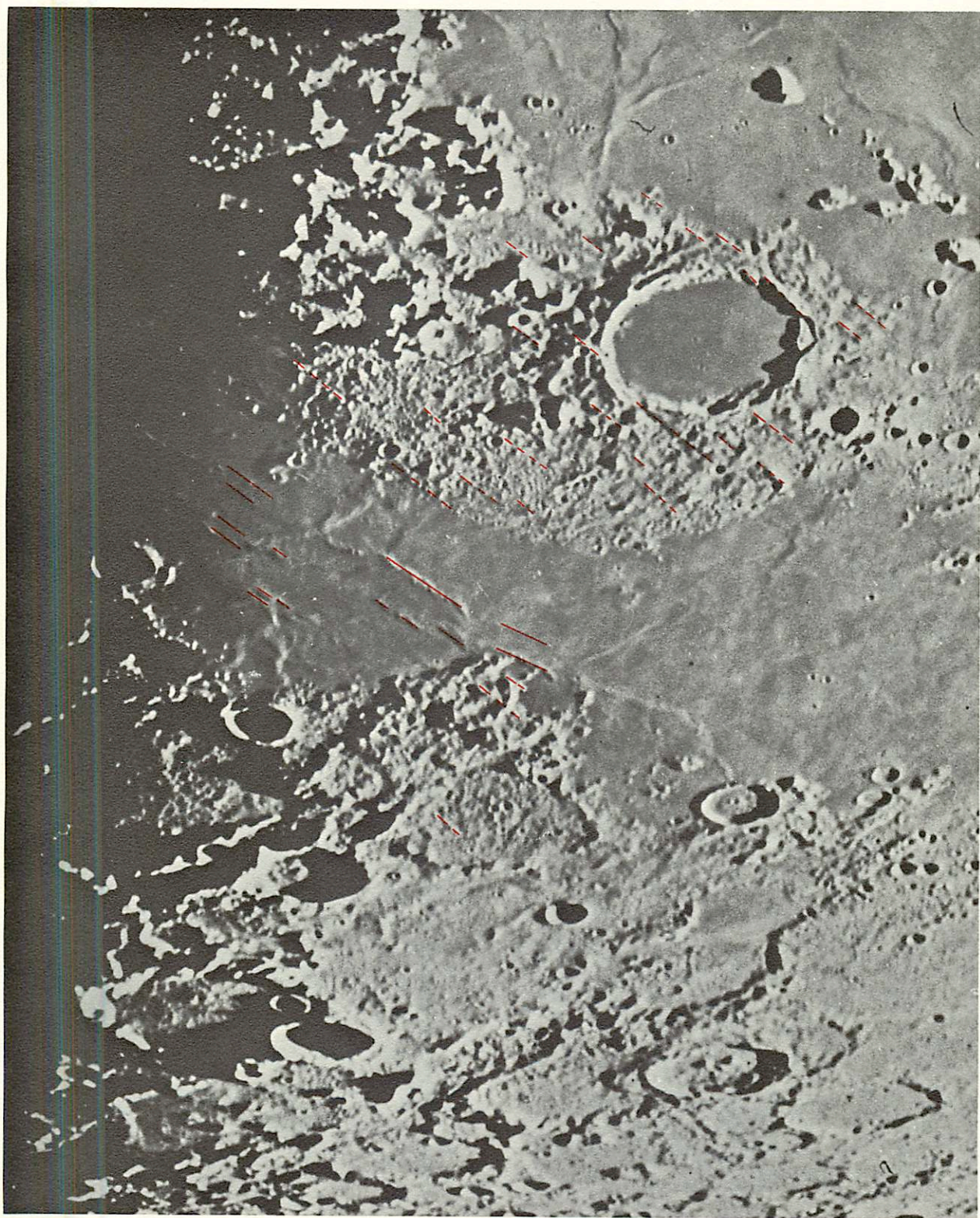


Plate 1b. Same as *1a*, with overlay marking parallelism between ridges and lineaments.

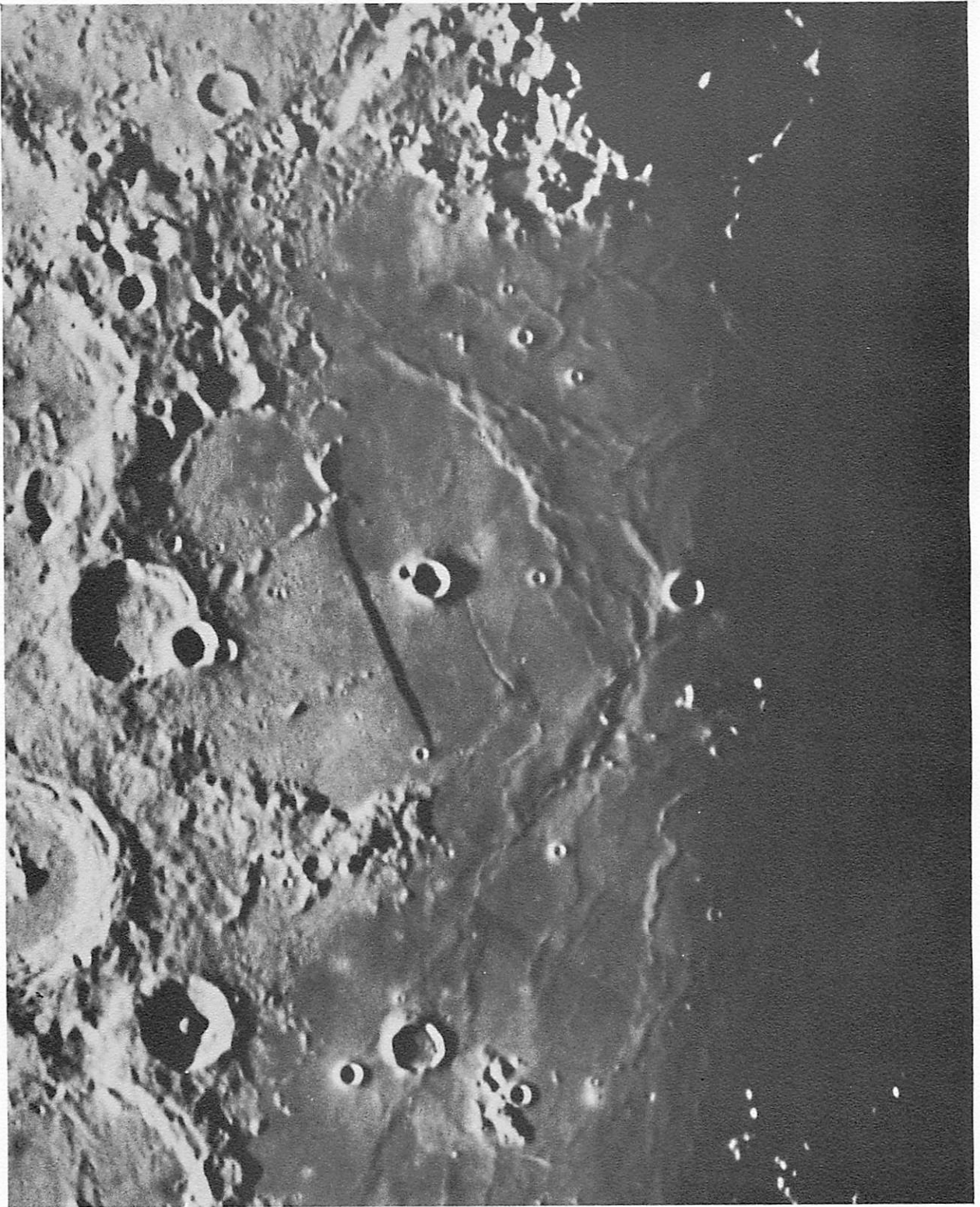


Plate 2a. Linear mare ridges in Mare Nubium which coincide with the direction of lineaments in the adjacent terrae.

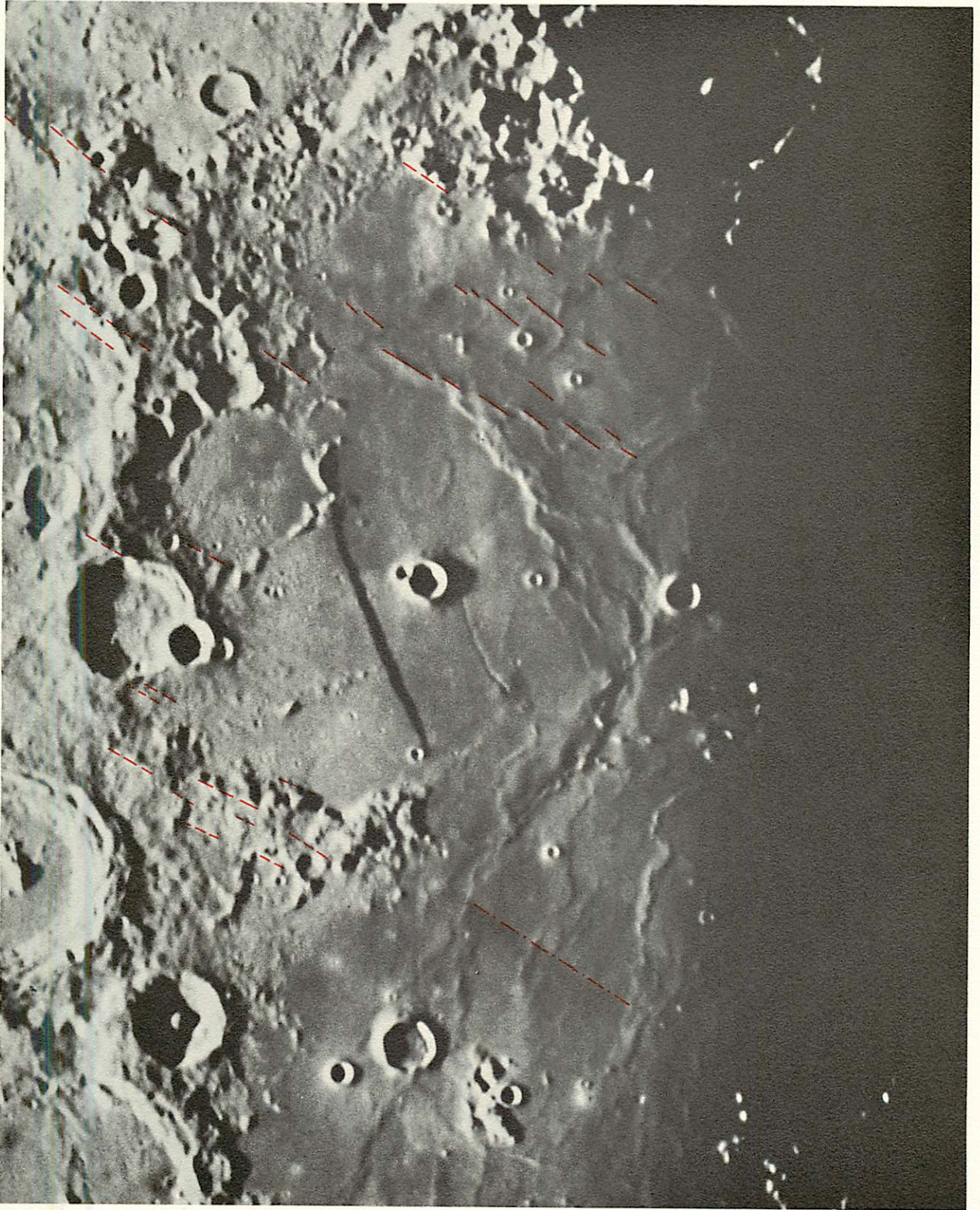


Plate 2b. Same as *2a*, with overlay marking parallelism between ridges and lineaments.

TABLE OF CONTENTS

No. 36	Radial Structures Surrounding Lunar Basins, II: Orientale and Other Systems; Conclusions.....	175
	by William K. Hartmann	
No. 37	Comparison of the Infrared Spectrum of Mars with the Spectra of Selected Terrestrial Rocks and Minerals.....	193
	by Alan B. Binder and Dale P. Cruikshank	
No. 38	On the Distribution of Lunar Crater Diameters.....	197
	by William K. Hartmann	
No. 39	Analysis of Lunar Lineaments, I: Tectonic Maps of the Moon.....	205
	by Robert G. Strom	